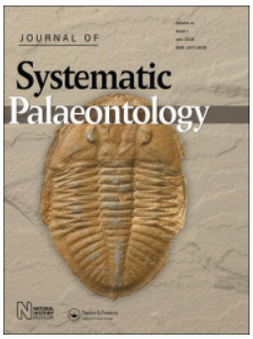

Journal of Systematic Palaeontology

ISSN: (Print) (Online) Journal homepage: https://www.tandfonline.com/loi/tjsp20

The oldest fossil record of *Bauhinia* s.s. (Fabaceae) from the Tibetan Plateau sheds light on its evolutionary and biogeographic implications

Yi Gao, Ai Song, Wei-Yu-Dong Deng, Lin-Lin Chen, Jia Liu, Wei-Cheng Li, Gaurav Srivastava, Robert A. Spicer, Zhe-Kun Zhou & Tao Su

To cite this article: Yi Gao, Ai Song, Wei-Yu-Dong Deng, Lin-Lin Chen, Jia Liu, Wei-Cheng Li, Gaurav Srivastava, Robert A. Spicer, Zhe-Kun Zhou & Tao Su (2023) The oldest fossil record of *Bauhinia* s.s. (Fabaceae) from the Tibetan Plateau sheds light on its evolutionary and biogeographic implications, Journal of Systematic Palaeontology, 21:1, 2244495, DOI: 10.1080/14772019.2023.2244495

To link to this article: https://doi.org/10.1080/14772019.2023.2244495

Journal of Systematic Palaeontology, 2023
Vol. 21, No. 1, 2244495
http://dx.doi.org/10.1080/14772019.2023.2244495

Taylor & Francis
Taylor & Francis Group

The oldest fossil record of *Bauhinia* s.s. (Fabaceae) from the Tibetan Plateau sheds light on its evolutionary and biogeographic implications

Yi Gao[a,b], Ai Song[a,c], Wei-Yu-Dong Deng[a,d], Lin-Lin Chen[e], Jia Liu[a,b], Wei-Cheng Li[a,b], Gaurav Srivastava[f], Robert A. Spicer[a,g], Zhe-Kun Zhou[a] and Tao Su[a,b]*

[a]*CAS Key Laboratory of Tropical Forest Ecology, Xishuangbanna Tropical Botanical Garden, Chinese Academy of Sciences, Mengla 666303, Yunnan, PR China;* [b]*University of Chinese Academy of Sciences, Beijing 100049, PR China;* [c]*Institute of Palaeontology, Yunnan Key Laboratory of Earth System Science, Yunnan Key Laboratory for Palaeobiology, MEC International Joint Laboratory for Palaeobiology and Palaeoenvironment, Yunnan University, Kunming 650500, PR China;* [d]*Paleontology Section, Institute of Geoscience, Rheinische Friedrich-Wilhelms Universität Bonn, Bonn 53115, Germany;* [e]*School of Geographical Sciences, University of Bristol, Bristol, BS81QU, UK;* [f]*Cenozoic Palaeofloristic Megafossil Lab, Birbal Sahni Institute of Paleosciences, Lucknow 226 007, India;* [g]*School of Environment, Earth and Ecosystem Sciences, The Open University, Milton Keynes MK7 6AA, UK*

(Received 20 March 2023; accepted 28 July 2023)

Bauhinia s.s. is a large genus in the family Fabaceae, but its evolutionary and biogeographical history is still unclear due to the scarcity of fossil records compared to the highly diverse modern species in pantropic regions. Here, we report the earliest fossil record of *Bauhinia* s.s., namely *Bauhinia tibetensis* Y. Gao et T. Su sp. nov., based on leaves from the latest Paleocene of the southern Tibetan region. Combined with palaeoecological niche simulations and ancestral state reconstruction, the new fossils suggested a Paleocene origin of *Bauhinia* s.s. in the Afrotropical realm that subsequently dispersed to the Neotropical and Indomalayan realms. *Bauhinia tibetensis* belongs to the Asian clade of *Bauhinia* s.s. that reached the southern Tibetan region from the Afrotropical realm via the Kohistan-Ladakh Island Arc in the early Paleocene. This clade spread to south-eastern China during the Oligocene and entered northern India during the Neogene or earlier. The discovery of the oldest *Bauhinia* s.s. from what is now the southern Tibetan Plateau updates our understanding of the biogeographical history of this genus and demonstrates that the Kohistan-Ladakh Island Arc is an ancient corridor for floristic interchange between Africa and India.

Keywords: *Bauhinia* s.s.; biogeography; diversification; Paleocene; leaf fossil; palaeoecological niche simulations

Introduction

Bauhinia s.l. is a large and taxonomically complex group in Cercidoideae (a subfamily of the Fabaceae), with nearly 380 living species (Sinou et al., 2020), encompassing trees, shrubs, lianas and herbs, mainly distributed in the Pantropical regions (Jia et al., 2022; Lin et al., 2015; Sinou et al., 2009). Among them, some species are famous horticultural plants worldwide, e.g. *Bauhinia acuminata* (Mak et al., 2008). *Bauhinia* s.l. includes a unique form that may be two-lobed with a prominent apical incision, or in other cases bifoliolate laminae (Chen & Zhang, 2005; Jia et al., 2022; Lin et al., 2015; Meng et al., 2014). Recent molecular studies have divided *Bauhinia* s.l. into 11 genera (i.e. *Bauhinia* s.s., *Phanera*, *Brenierea*, *Piliostigma*, *Barklya*, *Cheniella*, *Gigasiphon*, *Lasiobema*, *Lysiphyllum*, *Schnella* and *Tylosema*) (Sinou et al., 2009, 2020). Within the latest classification, *Bauhinia* s.s. is still a large genus (Sinou et al., 2020). Although extant *Bauhinia* species are diverse and wide in distribution, their fossil records are limited (Fig. 1; Supplemental material - Appendix 1). Hitherto, the oldest fossil record, namely *Bauhinia wenshanensis* and *Bauhinia* sp. (morphotypes 2–4), was from the late Eocene Puyang Basin in south-eastern Yunnan, China (Jia et al., 2022). Several fossil records from the Oligocene of China have been reported, including *Bauhinia wenshanensis* (Meng et al., 2014), *Bauhinia ningmingensis* (Wang et al., 2014), and *Bauhinia larsenii* (Chen & Zhang, 2005). Neogene fossil records are relatively richer than those of the Paleogene and include the Miocene *Bauhinia kachchhensis* (Lakhanpal & Guleria, 1982), *Bauhinium palaeomalabaricum* (Prakash & Prasad, 1984; Shukla et al., 2015), *Bauhinia* sp. cf. *B. purpurea* (Bande & Srivastava, 1988), *Bauhinia tertiara* (Awasthi & Mehrotra, 1989), *Bauhinia krishnanunnii* (Guleria et al., 2000) and *Bauhinia miocenica* (Mehrotra et al., 2011) discovered in India; *Bauhinia fotana* (Jacques et al., 2015) and *Bauhinia ungulatoides* (Lin et al., 2015) in

*Corresponding author. Email: sutao@xtbg.org.cn

Published online 17 Oct 2023

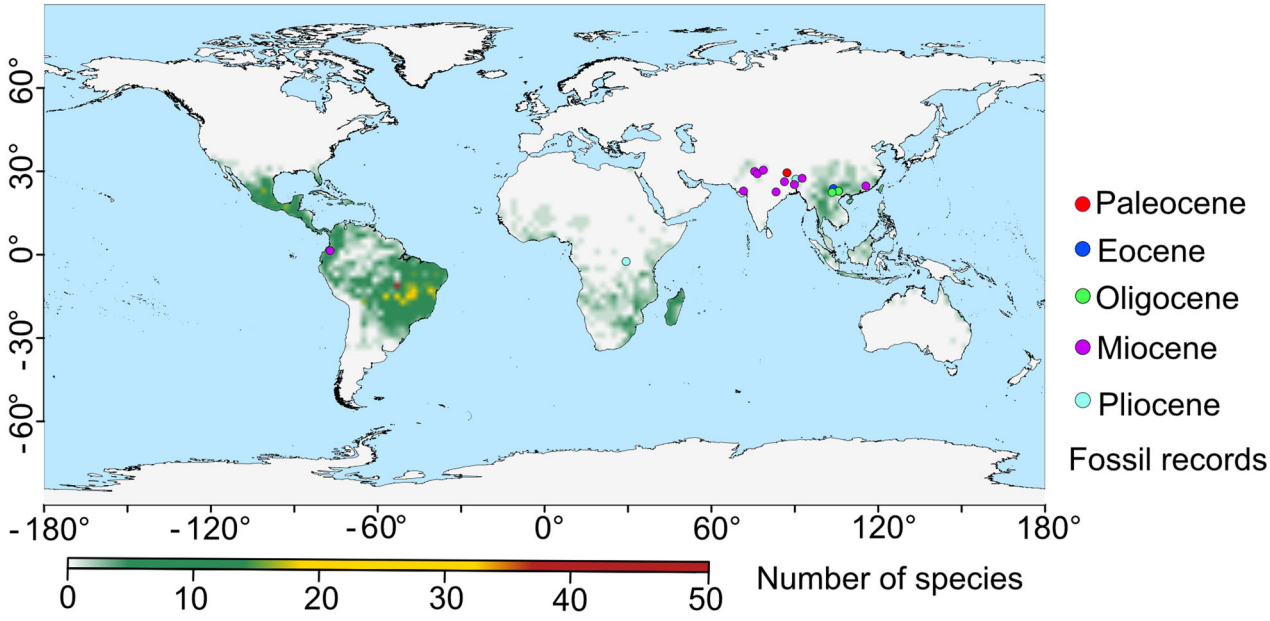

Figure 1. Modern and fossil distribution of *Bauhinia* s.s. Extant distribution data of *Bauhinia* s.s. were extracted from the Global Biodiversity Information Facility (GBIF, http://www.gbif.org) (Supplemental material - Appendix 2).

China; and *Bauhinia ecuadorensis* (Berry, 1945) discovered in Ecuador. The middle Miocene to Pliocene fossil record comprises *Bauhinia nepalensis*, from Nepal (Awasthi & Prasad, 1989), while Pliocene fossil records, namely *Bauhinia siwalika* (Khan et al., 2019) and *Bauhinia waylandi* (Chaney, 1933) are from India and Uganda, respectively.

Phylogenetic analysis and fossil records suggest that *Bauhinia* s.l. might have originated in Laurasia during the Paleocene (Meng et al., 2014); however, the age of the fossil species *Bauhinia wenshanensis* placed as a representative of the crown node in that study has been revised from the late Miocene to the early Oligocene based on radiometric dating (Tian et al., 2021). Moreover, the phylogenetic relationships within *Bauhinia* s.l. have also been revised in the latest analyses based on molecular data (Sinou et al., 2020). Therefore, any new fossil records of *Bauhinia* s.s., especially early occurrences, could significantly improve our understanding of the origin and evolution of this genus.

The Tibetan Plateau, the highest plateau on Earth, experienced drastic topographic and environmental changes, from warm and relatively low elevations in the Paleogene to the present high plateau (Spicer et al., 2021). Because the plateau landscape did not exist during the Paleogene, we use the term 'Tibetan region' instead of the Tibetan Plateau in this study. The Tibetan region played an important role in the evolution of Asian or even global plant diversity during the Cenozoic (Su et al., 2020), and recent fossil discoveries suggest that the Tibetan region was a crossroads for floristic interchange in the Northern Hemisphere (Deng et al., 2020; Liu et al., 2019; Zhou et al., 2023). Currently, however, the fossil record is still not sufficient to reveal the important roles that the Tibetan region played in the evolution and biogeographical history of the plants there, or even globally.

In this study, we report the oldest fossil record of *Bauhinia* s.s. in the form of leaves collected from the upper Paleocene Liuqu Formation, Lazi County, southern Tibet. These leaf fossils are assigned as a new species following detailed morphological comparison with living and previously reported fossil species. Furthermore, with this new fossil evidence, we reconstruct the evolutionary and biogeographic histories of *Bauhinia* s.l. and emphasize the importance of the Tibetan region and Kohistan-Ladakh Island Arc during the early stages of its dispersal.

Material and methods

Geological setting

The fossil site is located in Liuxiang, Lazi County (29.15° N, 88.15° E, ~4160 m above sea level), Xigaze, southern Tibet, China, which tectonically belongs to the Tethys Himalaya in the southern Tibetan Plateau. Fossil specimens were collected from the Liuqu Formation (Ding et al., 2017; Fang et al., 2005; Tao et al., 1988), also known as the Liuqu Conglomerate, which mainly

consists of thick coarse clastic rocks derived from the passive terrestrial margin of the Indian Plate and the ophiolites in the Yarlung-Zangpo suture (YZS), recording the tectonic evolution of the southern Tibetan region (Davis et al., 2002; Ding et al., 2017; Fang et al., 2005; Leary et al., 2016). The formation is restricted to an east–west elongated zone along the southern margin of the YZS, extends approximately 150 km, and varies in width from hundreds of metres to kilometres (Ali & Aitchison, 2008; Ding et al., 2017). It was formed by fluvial and sediment-gravity flow and is locally interbedded with mature paleosols (Leary et al., 2016). The fossils were collected from a fine sandstone layer in the upper part of the section (Fig. 2). The age estimated for the Liuqu Formation has been controversial and has ranged from Cretaceous to early Miocene (Davis et al., 2002; Ding et al., 2017; Fang et al., 2005; Leary et al., 2016, 2017; Li et al., 2015). However, Ding et al. (2017) conducted U-Pb dating with zircons from tuffite samples in the upper part of Liuqu Formation and constrained the age of Liuqu flora to approximately 56 Ma. Younger ages (Leary et al., 2017) are likely from Miocene dikes that crosscut the Liuqu Formation. Previously, plentiful fern and angiosperm fossils, such as *Christella nervosa*, *Annona prercticulata* and *Ficus protobenjamina*, have been discovered (Fang et al., 2005; Tao, 1988; Xu et al., 2019), indicating a subtropical to tropical environment.

Morphological observation

This study used a Nikon D850 camera for photography and a Leica S8APO stereomicroscope for fossil observation. The terminology of leaf architecture follows Hickey (1973) and Ellis et al. (2009). Ninety-four living species represented by 643 specimens (Supplemental material - Appendix 3) were obtained from the databases of the Chinese Virtual Herbarium (CVH, https://www.cvh.ac.cn) and Royal Botanic Gardens, Kew (http://apps.kew.org/herbcat/navigator.do) for morphological comparison. All plant scientific names we used strictly adhere to the unified standards of WFO Plant List (https://wfoplantlist.org/) to ensure consistency in nomenclature.

Geometric morphometrics

Geometric morphometrics (GMM) allows for the quantitative analysis and comparison of morphological differences among organisms (Bookstein, 1997; Klingenberg, 2022). In recent years, GMM has been widely used to analyse and compare quantitatively morphological differences among leaves of living species (Akli et al., 2022; Klein & Svoboda, 2017; Stojnić et al., 2022; Yang et al., 2022). More importantly, it has been shown to be an effective method for identifying fossil leaves when comparing spatial coordinate information of leaves with modern plant species (Chen et al., 2021; Meng et al., 2014).

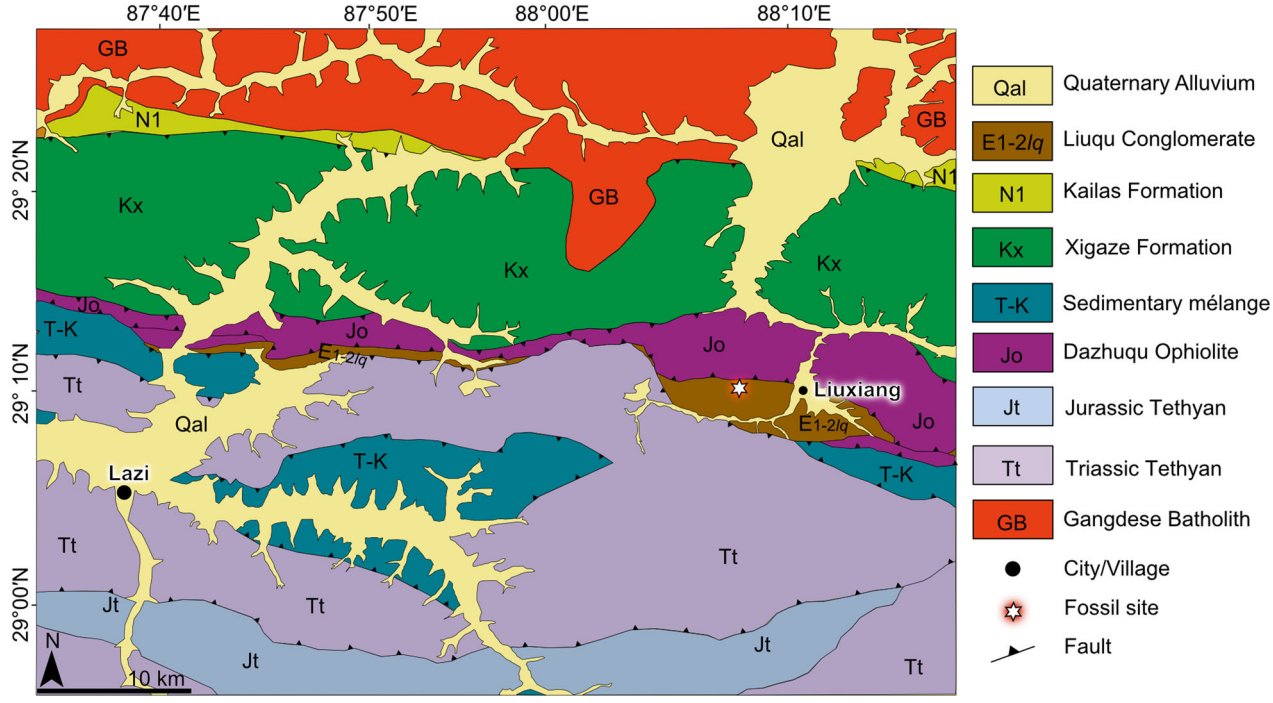

Figure 2. Geological map and fossil site in Liuxiang, Lazi County, Tibet (modified from Leary et al., 2016).

GMM was used to quantify morphological similarities among fossils and modern species of *Bauhinia* s.l. The steps for GMM are as follows:

1. Marking landmark and semi-landmark points. Landmark points are homologous points with distinct discriminatory features, and there are three types of landmark points for biological study. Type I landmark points are mainly the intersection points between different tissues, such as the intersection of primary veins and leaf margins; Type II is defined as depressions or protrusions in structures, such as leaf bases and leaf apices; Type III relates to the extreme values of the structure, such as the widest and longest points of the leaf blade. Semi-landmark points are a series of sliding points that outline biological contours and can add details to morphological variation. The software 'tps series' (Rohlf, 2015) can digitally analyse geometric morphometry, and this study used the software routines tpsUtil and tpsDig for image digitization. First, multiple specimen images of the same species are set into a single 'tps' file using tpsUtil. Then, the 'tps' file is opened with tpsDig to calibrate landmark and semi-landmark points to obtain coordinate information in the specimen images. Six landmark points were marked for each specimen containing type I or type II and 34 for the semi-landmarks (Fig. 5A). Steps 2–4 were all performed using the package 'geomorph' (Adams et al., 2020) in the software R to quantify the morphological variations and differences.
2. For statistical analyses, selected landmarks and semi-landmarks were transformed into morphological variables. The Generalized Procrustes Analysis (GPA) method was used to eliminate the nonmorphological variation through a series of processes involving rotation, angle adjustment, scaling and overprinting to align the corresponding points of each species as much as possible.
3. The interrelationship of morphological variation among specimens was explored by principal component analysis.
4. The obtained coordinate data were visualized on deformed grids using the thin-plate spline method to obtain ideal simulated images.

Phylogenetic analyses

We analysed the chloroplast gene tRNA-Leu (*trnL*) and the intergenic spacer *trnL-trnF* of 10 genera in *Cercidoideae* from GenBank (https://www.ncbi.nlm.nih.gov/nuccore, downloaded on 19 September 2022). The sequence data were compared, corrected, and sequenced using Aliview (v. 1.28) (Larsson, 2014). The tRNA-Leu (*trnL*) gene and *trnL-trnF* intergenic spacer sequence files in 'fasta' format were converted to 'nex' file format using ClustalX (v. 2.0) (Larkin et al., 2007). Then, the 'nex' file format was imported into the software PhyloSuite (v. 1.2.2) (Zhang et al., 2020), and the best-fit substitution model, GTR + F+G4 (Supplemental material - Appendix 4), was calculated by ModelFinder (Kalyaanamoorthy et al., 2017). After that, the sequence data in 'nex' format was imported into the software BEAUti (v. 1.10.4) (Suchard et al., 2018) to perform the node calibration, set priors and adjust relevant parameters. The marginal likelihood estimated by path sampling was used to compare the combinations of molecular clock models and coalescent models. The combination that best fit our data was the lognormal relaxed molecular clock model and Birth-Death Progress (Supplemental material - Appendix 5). Markov chain Monte Carlo (MCMC) was run for 10,000,000 generations and sampling was performed once every 1000 generations. The final 'xml' file exported from BEAUti was used in BEAST (v. 1.10.4) (Suchard et al., 2018) to generate trees. We used Tracer (v. 1.6) (Suchard et al., 2018) to check the effective sample size (ESS) of each 'log' file parameter, ensuring that ESS values (>200) achieved convergence. We kept 90% of the generated trees and discarded the first 10% of trees as burn-in by using Tree Annotator (v. 10.4) (Suchard et al., 2018) (Supplemental material - Appendix 6).

We set 66.0 Ma as the stem node of *Bauhinia* s.l. (Zhao et al., 2021) and placed one fossil calibration point (56.0 Ma), the earliest fossil record of *Bauhinia* s.s., namely *Bauhinia tibetensis*, reported here as a representative of the crown node for *Bauhinia* s.s.

Biogeographical analyses

According to the natural distribution patterns of *Bauhinia* s.l., four major regions were considered for biogeographical analysis (Supplemental material - Appendix 7): (A) the Indomalayan realm, (B) the Neotropical realm, (C) the Afrotropical realm and (D) the Australasian realm (Olson et al., 2001). The ancestral states were reconstructed by S-BGB (Statistical BAYAREALIKE in BioGeoBEARS) analysis in the software RASP (v. 4.2) (Matzke, 2014; Yu et al., 2020). The best fit biogeographic model statistical analysis of S-BGB was BAYAREALIKE + J (based on the highest AICc_wt: 0.25) (Supplemental material - Appendix 5). To minimize the influence of tree topology uncertainty on the reconstructed ancestral state, 2000 trees were randomly selected from 9000 trees calculated by BEAST (v. 1.10.4) (Suchard et al., 2018).

Palaeoecological niche model

We used the Hadley centre-coupled ocean-atmosphere general circulation models (HadCM3LBM2.1D) from the Hadley Centre (Met Office, UK) for palaeoclimate simulation (Valdes et al., 2017, 2021). Eight bioclimatic variables likely to be important for *Bauhinia* s.s. growth were selected, i.e. the coldest month mean surface air temperature (CMM), the coldest three continuous months mean surface air temperature (CSM), the driest month precipitation (DRYMON), the difference for wettest month-driest month precipitation (WETDRYMON), the wettest season precipitation (WETSEA), the warmest month mean surface air temperature (WMM), the warmest month-coldest month temperature difference (WMMCMM), and the warmest season-coldest season temperature difference (WSMCSM). We assume that these bioclimate variables for modern *Bauhinia* s.s. obtained from MaxEnt (v. 3.4.1) (Steven et al., 2022) have the same explanatory power for *Bauhinia* s.s. in the geological past. Each fossil record was checked, and their locations were transferred into palaeocoordinates to obtain accurate bioclimatic data. Palaeocoordinates were reconstructed using GPlates (https://gwsdoc.gplates.org/reconstruction) and based on the PALEOMAP palaeogeographic model of Scotese (2016). The extracted bioclimatic data for each corresponding epoch were aggregated as the total climatic range and were used as the climatic range of each period within that climatic group to construct the climatic ecological niche of each time bin. This method avoids the situation in which the climate range extracted in a certain time slice is too narrow due to the deficiency of fossil records in that period. Since each bioclimatic variable range in the same time bin projects to a different geographic area, the mask function of the R language 'Raster' package was used to obtain a common geographic area for these eight bioclimatic variables (Hijmans et al., 2020). The suitability of the climate for *Bauhinia* s.s. was evaluated using the Mahalanobis distance (MD), with values of MD = 0 representing the most suitable and values of MD = 1 representing the most unsuitable. We designed a value of MD < 0.25 for the most suitable potential distribution (MSPD) region for *Bauhinia* s.s.

Systematic palaeontology

Order **Fabales** Bromhead, 1838
Family **Fabaceae** Laurent de Jussieu, 1789
Subfamily **Caesalpinioideae** Pyramus de Candolle, 1825
Genus ***Bauhinia*** Plumier ex Linnaeus, 1753

Species ***Bauhinia tibetensis*** Y. Gao et T. Su sp. nov. (Figs 3, 4)

Holotype. XZLZLX1-0118 (Fig. 3I).

Paratypes. XZLZLX1-0106 (Fig. 3A, B), XZLZLX1-0112 (Fig. 3D, E), XZLZLX1-0119 (Fig. 3G), XZLZLX1-0110 (Fig. 4I), XZLZLX1-0415 (Fig. 4F), XZLZLX1-0417 (Fig. 4A), XZLZLX1-0418 (Fig. 4B), XZLZLX1-0420 (Fig. 4J, K), and XZLZLX1-0541 (Fig. 4E).

Material. The holotype and paratypes are deposited in the Paleoecology Collections of Xishuangbanna Tropical Botanical Garden, Chinese Academy of Sciences.

Type locality. Liuxiang village, Lazi County, Xigaze, Tibet, China (Fig. 2).

Etymology. The specific epithet '*tibetensis*' refers to the region where the species was found.

Type horizon. The upper part of the Liuqu Formation, late Paleocene; ~56 Ma.

Diagnosis. Leaf size microphyll to mesophyll, lamina orbicular to broadly elliptical, simple, bilobed, apex of each lobe round-obtuse, base round, or ovate. Veins actinodromous, primary veins 7–9, midvein ending at the sinus; secondary veins simply brochidodromous, terminating at leaf margin; tertiary veins mixed percurrent between secondary veins and primary veins.

Description. The leaf blade is suborbicular or broadly ovate, microphyll to mesophyll in size, symmetrical, bilobed, and both lobes are round at the apex (Figs 3G–J, 4B, D). The apex incision is approximately 1/6–2/5 of the blade length (Figs 3D, F, I, J, 4B, D). The petiole is not preserved. The leaf base is symmetrical, truncate to shallow cordate (Figs 3G–J, 4B, D, E, G). The lamina length is approximately 1.7–4.3 cm, the width is approximately 2.6–5.4 cm, the length-to-width ratios are approximately 0.5–0.8, and the blade area is approximately 4.2–19.7 cm^2 (Figs 3, 4). Primary veins are 7–9, not convergent toward the apex (Figs 3A–C, G–J, 4A–E, G). The angle between the main veins is consistent (Figs 3, 4). Simple agrophic veins are present (Fig. 3D, F–H). The midvein is straight and ends at the sinus (Figs 3A–C, I, J, 4A–D). Secondary veins are simple brochidodromous with inconsistent angles and irregular spacing (Figs 3, 4). Intersecondary veins occasionally have less than one intersecondary vein in each interval (Fig. 4J–L). The tertiary veins are mixed percurrent between the secondary veins and the main veins (Fig. 4J–L). Higher-order veins are not preserved.

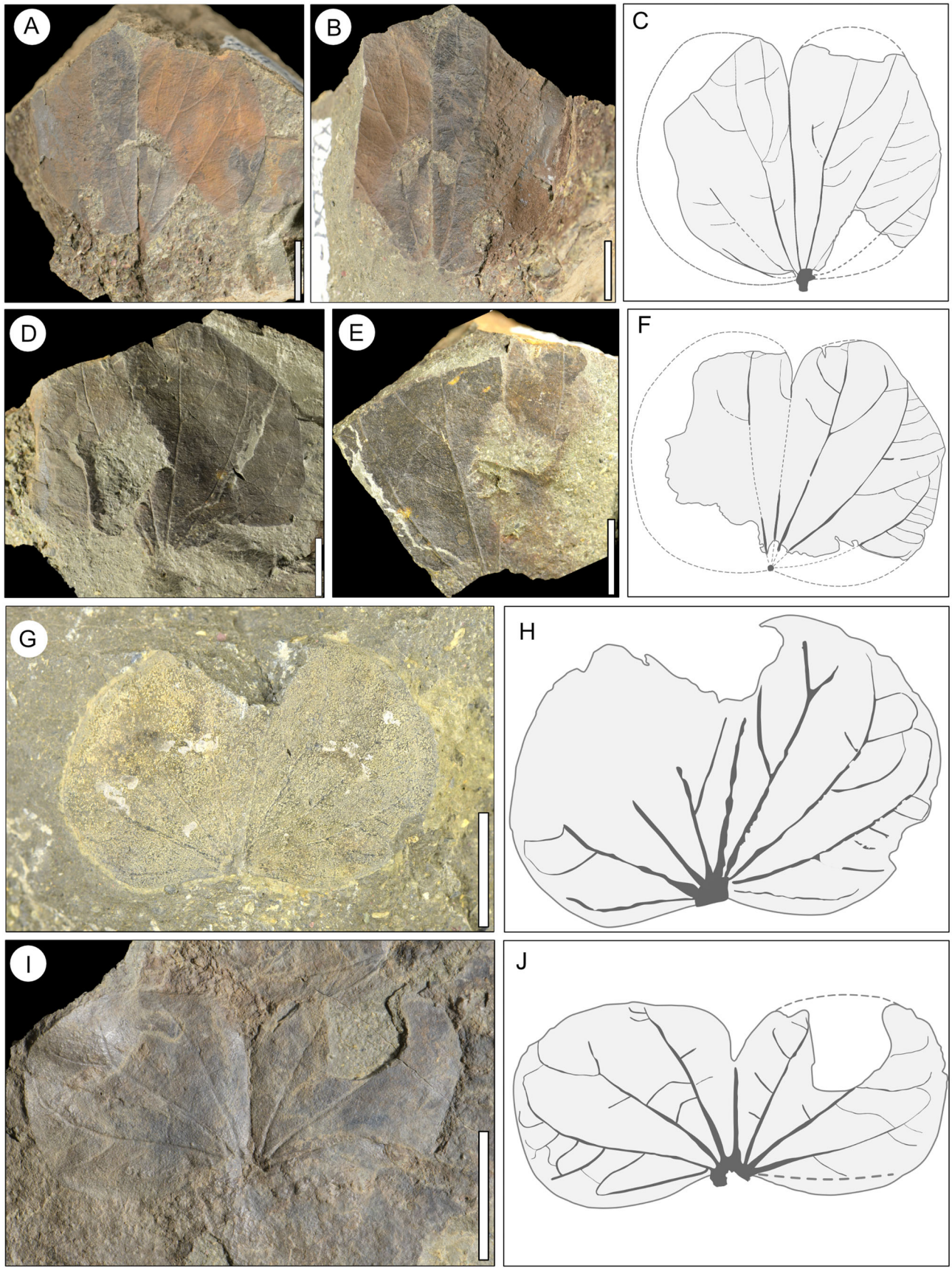

Figure 3. Fossil leaves and line drawings of *Bauhinia tibetensis* Y. Gao et T. Su sp. nov. from the Upper Liuqu Formation, Liuxiang village, Lazi County, Xigaze City, Tibet, China. **A,** XZLZLX1-0106; **B,** XZLZLX1-0106 (counterpart); **C,** line drawing of A; **D,** XZLZLX1-0112; **E,** XZLZLX1-0112 (counterpart); **F,** line drawing of D; **G,** XZLZLX1-0119; **H,** line drawing of G; **I,** XZLZLX1-0118; **J,** line drawing of I. Scale bars equal 1 cm.

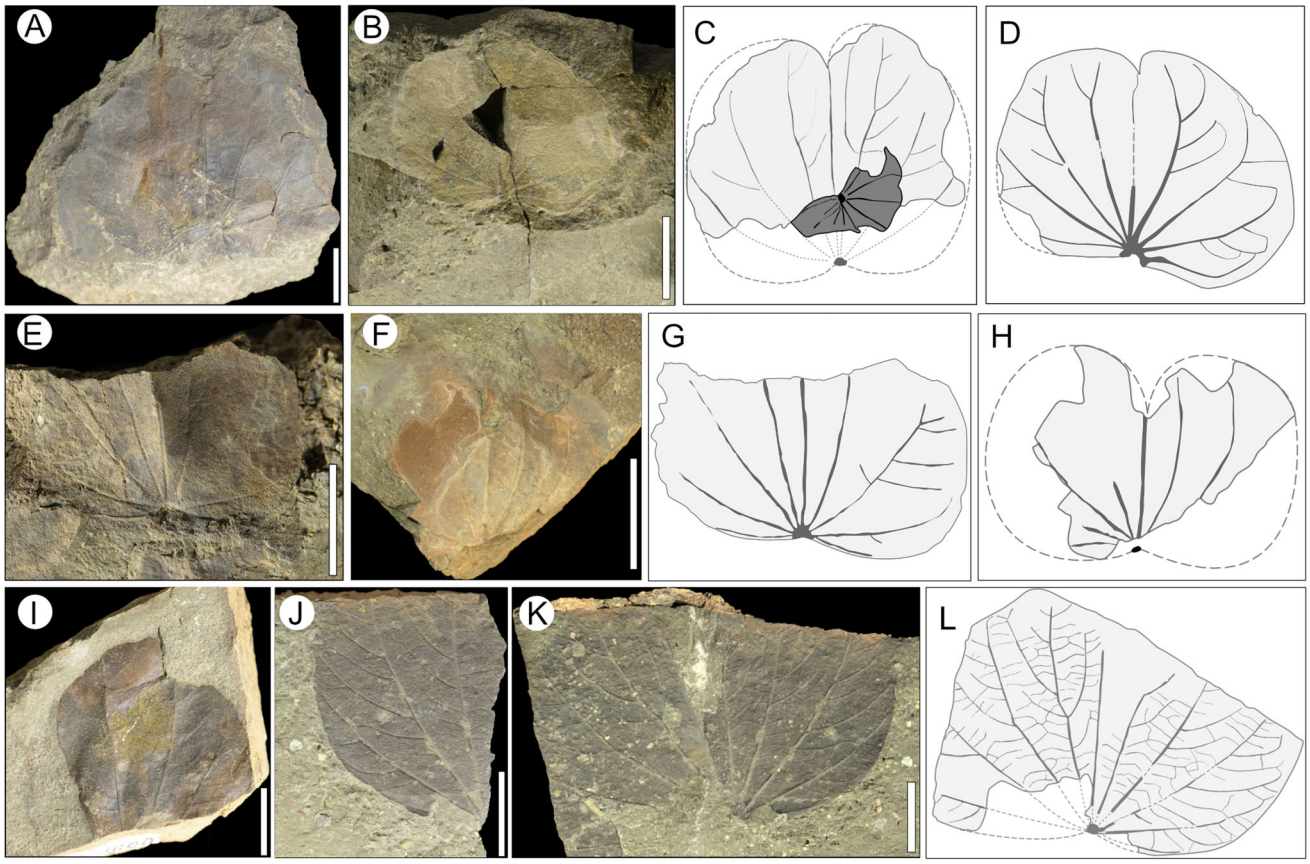

Figure 4. Fossil leaves and line drawings of *Bauhinia tibetensis* Y. Gao et T. Su sp. nov. from the Upper Liuqu Formation, Liuxiang village, Lazi County, Xigaze City, Tibet, China. **A,** XZLZLX1-0417; **B,** XZLZLX1-0418; **C,** line drawing of A; **D,** line drawing of B; **E,** XZLZLX1-0541; **F,** XZLZLX1-0415; **G,** line drawing of E; **H,** line drawing of F; **I,** XZLZLX1-0110; **J,** XZLZLX1-0420; **K,** XZLZLX1-0420 (counterpart); **L,** line drawing of K. Scale bars equal 1 cm.

Results

Leaf geometry and morphometric pattern

The results of the principal component analysis of the interrelationships of leaf shape among modern and fossil species of *Bauhinia* s.l. (Fig. 5) indicates that *Bauhinia* s.s., *Piliostigma*, *Phanera*, *Cheniella*, *Lysiphyllum*, *Schnella*, and *Tylosema* overlap in general leaf morphology. Nevertheless, their leaves could be distinguished by detailed morphological characters at the species level (Fig. 5). The first two principal components (PC1 and PC2) accounted for 76.61% of the total variables of leaf shape across samples (Supplemental material - Appendix 5). Thin-plate spline deformation grids (Fig. 5B) show that PC1 represents the common variation in width between two lobes and the depth of the base concavity, accounting for 53.80% of the total variables of leaf shape. PC2 represents the variation in the depth between the two lobes, apex shape, and the ratio of laminar length to width, accounting for 22.81% of the total variables of leaf shape (Fig. 5). From the PCA results, *B. tibetensis* was morphologically similar to *Cheniella damiaoshanensis* and *Bauhinia variegata*. However, when the size of the leaf blade and the number and structure of the leaf veins were considered, *B. tibetensis* was the closest to *B. variegata* in morphology.

Phylogenetic relationships and divergence times

According to our analyses, with the assignment of 66.0 Ma as the stem node, the divergence age of *Bauhinia* s.l. was in the earliest Paleocene (*ca*. 65.3 Ma, 95% Highest Posterior Density (HPD): 62.8–66.8 Ma), with the clade of *Bauhinia* and *Phanera* diverged by 63.0 Ma (95% HPD: 60.3–65.5 Ma). In the *Bauhinia* clade, *Bauhinia* s.s. had diverged by 59.7 Ma (95% HPD: 57.0–62.6 Ma); then, the Asian and American-African clades diverged by 55.8 Ma (95% HPD: 54.9–56.8 Ma). In the middle Eocene (45.3 Ma, 95% HPD: 29.68–55.69 Ma), it diverged into the American and African clades (Fig. 6).

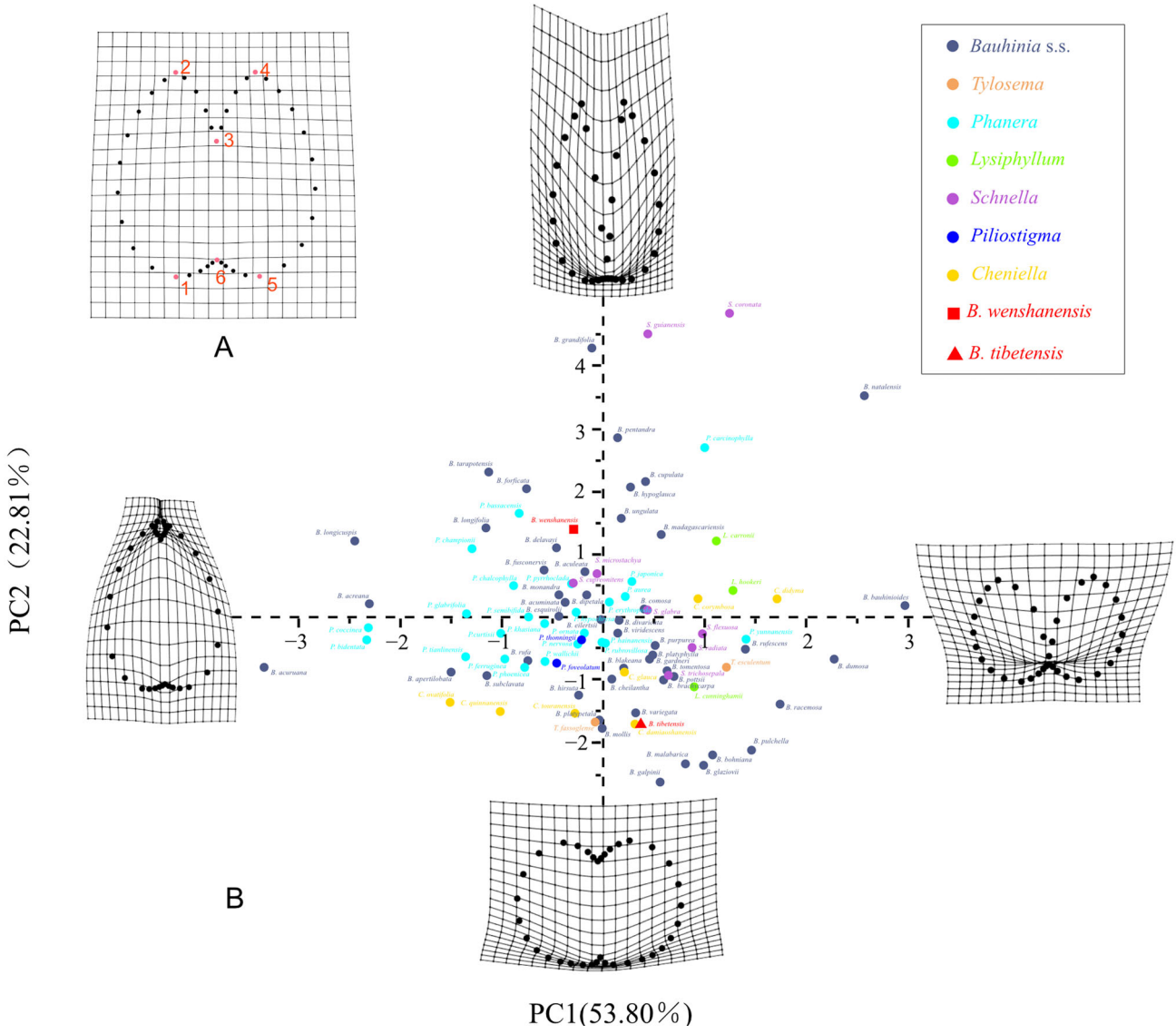

Figure 5. Principal component analysis and range of leaf shape within two fossil species, namely *B. tibetensis* and *B. wenshanensis*, and living species of *Bauhinia* s.l. **A,** position and description of landmarks and semi-landmarks. **B,** distribution of specimens according to the first principal component (53.80% variability) and the second principal component (22.81% variability). Different colours represent different genera in *Bauhinia* s.l. Red triangle represents *Bauhinia tibetensis*. Red square represents *Bauhinia wenshanensis*. The thin-plate spline deformation grid represents the leaf shapes corresponding to the most positive (+) and negative (–) principal component scores.

Biogeographical reconstruction

Most *Bauhinia* species are distributed in tropical and subtropical regions. There are three modern distribution centres: south-east Asia, South America, and South Africa (Fig. 1). An ancestral state reconstruction was conducted in RASP 4.2, and the results showed that the most recent common ancestral distribution range of *Bauhinia* s.l. is probably in the Afrotropical realm (98.5%, node: 85). The ancestral distribution of divergent clades of *Bauhinia* and *Phanera* is also probable in the Afrotropical realm (98.3%, node: 83), followed by *Bauhinia* s.s., *Brenierea* and *Piliostigma*, which also probably originated there (98.7%, node: 67). The ancestral state of the crown *Bauhinia* s.s. (node 64 in Fig. 4) is most likely to be in the Afrotropical realm (90.0%), followed by Asia (6.5%). This result suggested that the early divergence of *Bauhinia* s.l. took place in the Afrotropical realm. For the *Bauhinia* clade, it was not until the divergence of *Bauhinia* s.s. that it spread out of the Afrotropical realm.

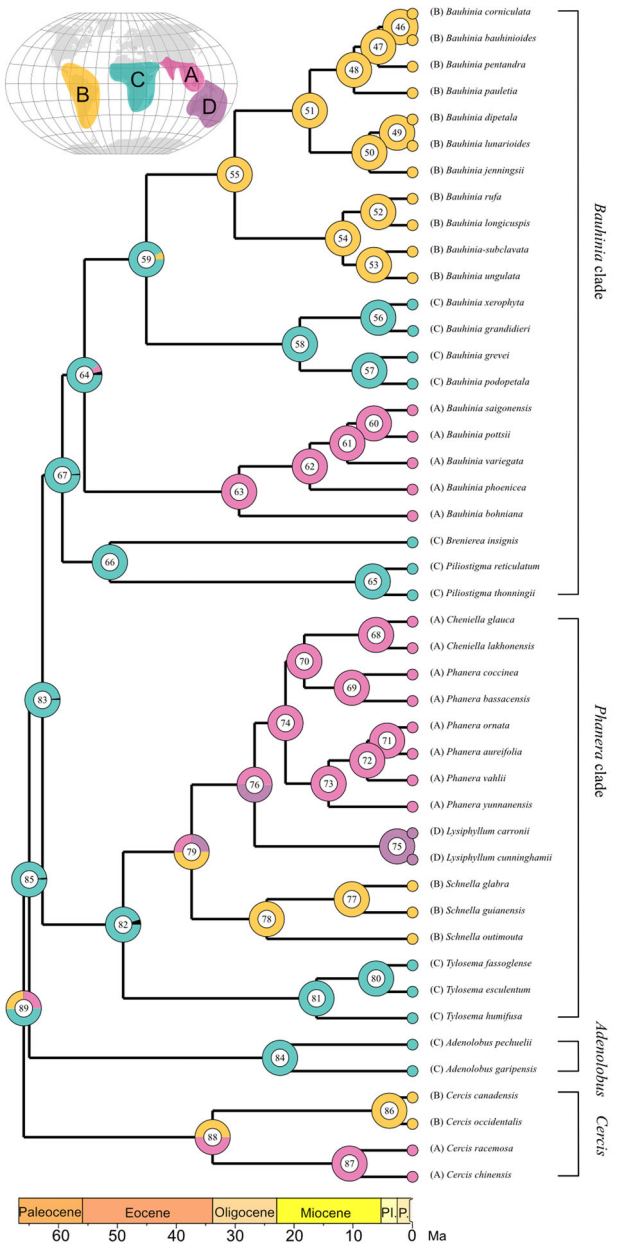

Figure 6. Ancestral distributions at each node of the phylogeny of Caesalpinioideae obtained by S-BGB. Each pie chart indicates the probabilities of distribution. Numbers represent nodes (46–89). The colour of each node represents the distribution range: **A,** the Indomalayan realm; **B,** the Neotropical realm; **C,** the Afrotropical realm; and **D,** the Australasian realm.

Historical distribution of *Bauhinia* s.s

For extant *Bauhinia* s.s., the MaxEnt model results (Supplemental material - Appendix 8) show that temperature is amongst the most important factors limiting the natural distribution of *Bauhinia* s.s. The possible temperature range for survival of *Bauhinia* s.s. corresponds to CSM between 16 °C and 25 °C and WSMCSM between 2 °C and 7 °C. It indicates that *Bauhinia* s.s. preferred regions with high temperatures in winter and small temperature differences between the warmest and coldest seasons. Precipitation factors, especially WETDRYMON and WETMON, also play crucial roles in affecting the survival of *Bauhinia* s.s. A WETMON higher than 140 mm makes it suitable for *Bauhinia* s.s. to grow, while a DRYMON higher than 38 mm makes it possible for *Bauhinia* s.s. to grow.

Using the palaeoecological niche model, the potential distribution of *Bauhinia* s.s. was reconstructed for each Cenozoic epoch (Fig. 7). During the Paleogene, the most suitable potential distribution (MSPD) of *Bauhinia* s.s. extended across the whole pantropical area (Fig. 7A, B), and some even entered higher latitudes in Asia. In the Miocene, the MSPD of *Bauhinia* s.s. was limited in low latitudes, and a wide potential distribution existed in Africa (Fig. 7C). A further contraction of the MSPD occurred during the Pliocene, but *Bauhinia* s.s. persisted within a pantropical distribution (Fig. 7D).

Discussion

Morphological comparison

We classified species in *Bauhinia* s.l. using leaf shape, apex, base, and the number of primary veins (Supplemental material - Appendix 5). *Piliostigma* has five living species. Among them, the leaves of *P. foveolatum*, *P. reticulatum*, *P. thonningii* and *P. tortuosum* are macrophyll, significantly larger than fossils from Lazi County, and the leaves of *P. malabaricum* are microphyll to mesophyll with two round apexes, but the base is deeply cordate. Leaves in *Lysiphyllum* are 2-foliolate or unlobed, and leaves in *Barklya* and *Gigasiphon* are both unlobed. For leaves of *Schnella*, the base is deeply cordate, and the apex is usually acuminate to straight. In *Cheniella*, the leaf blade shape of *C. damiaoshanensis* is similar to our fossils, but *C. damiaoshanensis* has only seven primary veins. Most species in *Phanera* show acute or acuminate leaf apices. Although the leaf apex in a few *Phanera* species is round or obtuse, their leaf base is deeply cordate (e.g. *P. semibifida* and *P. yunnanensis*).

Bauhinia s.s. is a large genus with a wide range of leaf shapes, such as 2-foliolate (e.g. *B. divaricata*, *B. grevei*, *B. bauhinioides*, unlobed (e.g. *B. cinnamomea*, *B. brachycalyx*, *B. acuruana*), the apex is acuminate or straight (e.g. *B. aculeata*, *B. decandra*, *B. esquirolii*), the apex is round with deeply cordate base (e.g. *B. galpinii*, *B. racemosa*, *B. ellenbeckii*), and the apex is round with deeply bilobed (e.g. *B. leucantha*, *B. morondavensis*, *B. grandidieri*). After checking 47 species represented by 354 specimens (Supplemental material -

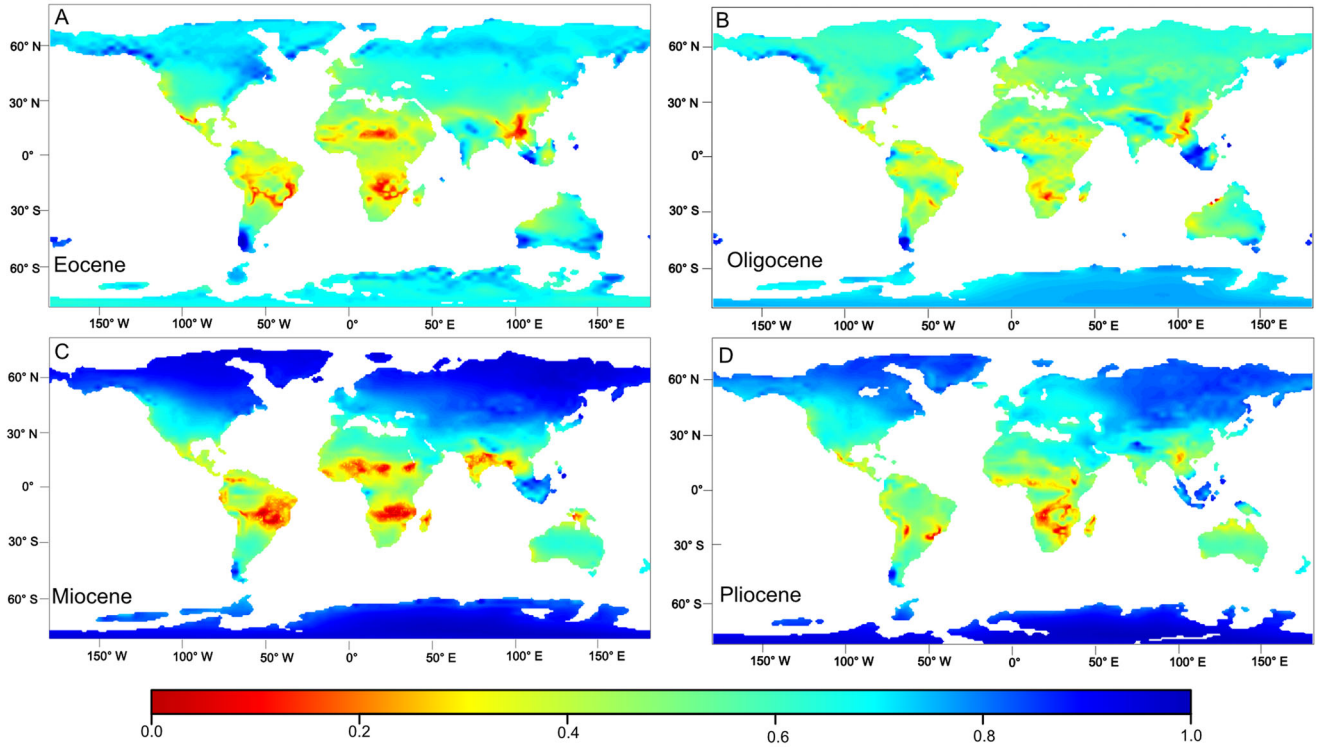

Figure 7. Potential distribution regions of *Bauhinia* s.s. from the Eocene to Pliocene based on key climatic parameters. Mahalanobis distance (MD) from 0 to 1 indicates the most suitable to the least suitable distribution of *Bauhinia* s.s.

Appendix 3), we found that *B. variegata* is quite similar to our fossil specimens. Both have a shallow cordate, sometimes truncated base and two round apices, the leaf shape is broadly ovate to round, and the width of the leaf blade is usually longer than the length.

In addition, we performed morphometric analysis among *Bauhinia* s.l. and our fossils (Fig. 5). The results suggest that the apex shape, the depth and width of the bilobation, and the base shape are the main characters that express 76.6% of the leaf shape variation in *Bauhinia* s.l. We also found that *B. variegata* closely resembles fossils from Lazi County (Fig. 5). Nevertheless, those fossils still have some morphological differences from *B. variegata*, as evidenced by the 7–9 primary veins in our fossils compared to 9–13 in *B. variegata*.

To date, 14 leaf fossil species supposedly representing *Bauhinia* s.l. have been reported worldwide (Jia et al., 2022). Among them, nine species, namely *B. waylandi*, *B. wenshanensis*, *B. ningmingensis*, *B. cheniae*, *B. fotana*, *B. ungulatoides*, *B. ecuadorensis*, *B. nepalensis* and *Bauhinia* sp. cf. *B. purpurea* present two straight apexes (Awasthi & Prasad, 1989; Bande & Srivastava, 1988; Berry, 1945; Chaney, 1933; Jacques et al., 2015; Jia et al., 2022; Lin et al., 2015; Meng et al., 2014; Wang et al., 2014). Two fossil species show round leaf apices and are deeply bilobed, namely *Bauhinia larsenii* (Chen & Zhang, 2005), and *Bauhinia* sp. (morphotype 2–3) (Jia et al., 2022). *B. krishnanunnii* and *B. siwalika* are incomplete in that the apex and base of the leaf blade are not preserved (Guleria et al., 2000; Khan et al., 2019). Although the leaf shape of *Bauhcis moranii* from the Oligocene of Mexico is similar to that of *Bauhinia* s.s., the character of the secondary veins that rise from a midvein is close to that of *Cercis* (Calvillo-Canadell & Cevallos-Ferriz, 2002). In comparison, these leaf fossils from Lazi County are obviously different from any previously reported leaf records; therefore, we designated them as a new species, namely *Bauhinia tibetensis* Y. Gao et T. Su sp. nov.

Biogeographical implications

By palaeoecological niche model simulation, the MSPD of *Bauhinia* s.s. covered a wide range within the Indomalayan, Neotropical and Afrotropical realms during the Eocene (Fig. 7A). After the Eocene–Oligocene Transition (EOT), the global climate transformed from a warmhouse to a coolhouse (Westerhold et al., 2020; Zachos et al., 2001), which may have caused the MSPD of *Bauhinia* s.s. to undergo a significant latitudinal contraction in both the northern and southern hemispheres (Fig. 7B). During the Miocene, due to the high adaptability and tolerance of *Bauhinia* s.s. to climate change,

the MSPD of *Bauhinia* s.s. dramatically increased (Fig. 7C), especially during warm periods such as the middle Miocene Climate Optimum (MMCO) (Westerhold et al., 2020). In the Indomalayan realm, the MSPD expanded to India. During the Pliocene, the MSPD of *Bauhinia* s.s. disappeared in the Afrotropical realm probably due to the aridification of Africa after the late Miocene (Zhang et al., 2014), and the distribution of this genus emerged as a modern pattern at this time (Fig. 7D). Generally, although MSPD showed a fluctuating trend from the Eocene to the Pliocene, it has been consistently present in the Indomalayan, Neotropical and Afrotropical realms since the Eocene.

Modern *Bauhinia* s.s. species are widespread in Asia, Africa, and the Americas, but there is only one fossil record in Africa (namely *B. waylandi*) (Chaney, 1933) and the Americas, respectively (namely *B. ecuadorensis*) (Berry, 1945). The currently known earliest fossil record of *Bauhinia* s.s., namely *B. tibetensis* described here, is from the latest Paleocene (∼56 Ma) of the southern Tibetan region and provides crucial information on the evolution of *Bauhinia* s.s., especially in its early stage. We conducted Bayesian divergence time analyses of the subfamily Caesalpinioideae with the latest fossil and molecular evidence. The results indicated that *Bauhinia* s.s. may have diverged around 59.7 Ma, slightly younger than proposed by the previous study, which suggested a divergence time around 62.7 Ma for *Bauhinia* s.l. as a whole (Meng et al., 2014). Subsequent to their study, the age of the fossil species (namely *Bauhina wenshanensis*), used as the crown node, was reassigned from late Miocene to early Oligocene, ∼32.0 Ma (Tian et al., 2021) based on radiometric dating. Moreover, *Bauhinia yunnanensis* has been revised as *Phanera yunnanensis* (Sinou et al., 2020), which was considered to originate from Asia with evidence of the earliest divergence of *Bauhinia* s.s.

In this study, we simulated the MSPD of *Bauhinia* s.s. from the Eocene to Pliocene. However, given the global climate pattern throughout the Cenozoic, we suggest that the MSPD of *Bauhinia* s.s. may have been present in the Afrotropical realm since the Paleocene, which provided suitable environmental conditions for the origin of *Bauhinia* s.s. Other studies have also shown similar phenomena. For example, given that the earliest fossil record of Asclepiadoideae (Apocynaceae) was found in Tibet (Del Rio et al., 2020); molecular phylogenetic studies suggest that its centre of origin was in Africa (Del Rio et al., 2020; Rapini et al., 2003).

In addition, the ancestral state reconstruction indicates that *Bauhinia* s.s. probably diverged first in the Afrotropical realm (Fig. 6). Although *B. tibetensis* is the earliest fossil record worldwide to date, the results of ancestral state reconstruction suggest that the ancestral distribution of *Bauhinia* s.l. was likely in the Afrotropical realm (node: 85, 96.8%). By 63.0 Ma, *Bauhinia* s.l. diverged to form the clades of *Bauhinia* and *Phanera* locally in the Afrotropical realm, followed by *Bauhinia* s.s. at 59.7 Ma. Therefore, this study suggests that *Bauhinia* s.s. originated in the Afrotropical realm and experienced a floristic interchange pattern typical of the 'out of Africa' model.

This pattern is also supported by other fossils and phylogenetic evidence. Previous studies, such as that of Asclepiadoideae (Del Rio et al., 2020; Rapini et al., 2003), have indicated that floral interchange between the Afrotropical realm and Indomalayan realm already existed by the latest Paleocene. Our study of *B. tibetensis* provides further evidence for this interchange pattern. Additionally, the fruit fossils of *Illigera* found in the Jianglang flora of Tibet also provide important evidence suggesting this interchange between the Afrotropical realm and the Indomalayan realm in the Eocene (Wang et al., 2021).

The Kohistan-Ladakh Island Arc (KLIA) was an important dispersal corridor between Africa and India (Ali & Aitchison, 2008; Ashton et al., 2021; Chatterjee et al., 2013; Morley, 2018; Smith et al., 2016). For example, the biogeographic analysis based on pollen fossils suggests that Dipterocarpaceae originated from Africa during the mid-Cretaceous, and it spread to India through the KLIA during the Late Cretaceous to Paleocene (Bansal et al., 2022). The discovery of *B. tibetensis* further supports the existence of this passage: *Bauhinia* s.s. may spread from Africa via the KLIA to the southern Tibetan region by the late Paleocene, and then dispersed to Asia. During the late Paleocene, the southern Tibetan region was warm and no more than 1 km above mean sea-level (Ding et al., 2017), which should be suitable for the survival of *Bauhinia* s.s. After the closure of the north India Sea (Yuan et al., 2022), it dispersed to southern India.

The North Atlantic Land Bridge (NALB) has been regarded as one of the most important passages for Pantropical flora in the Paleogene of the Northern Hemisphere (Davis et al., 2002; Zhou et al., 2006, 2020). The leaf fossils of *Berhamniphyllum* (Rhamnaceae) reported from Markam in the south-eastern Tibetan region indicate that the group spread from the Neotropical realm to the Palearctic realm via the NALB and then into the Afrotropical realm during the middle Eocene (Zhou et al., 2020). Based on model simulation and palaeogeography, we suggest a potential migration route: *Bauhinia* s.s. followed the route of *Berhamniphyllum*, but in the opposite direction. It originated from the Afrotropical realm, spread toward the Mediterranean region, and then entered the Neotropical realm via the NALB after the early Oligocene (Fig. 8). Nonetheless, this hypothesis requires further substantiation with additional fossil evidence in future.

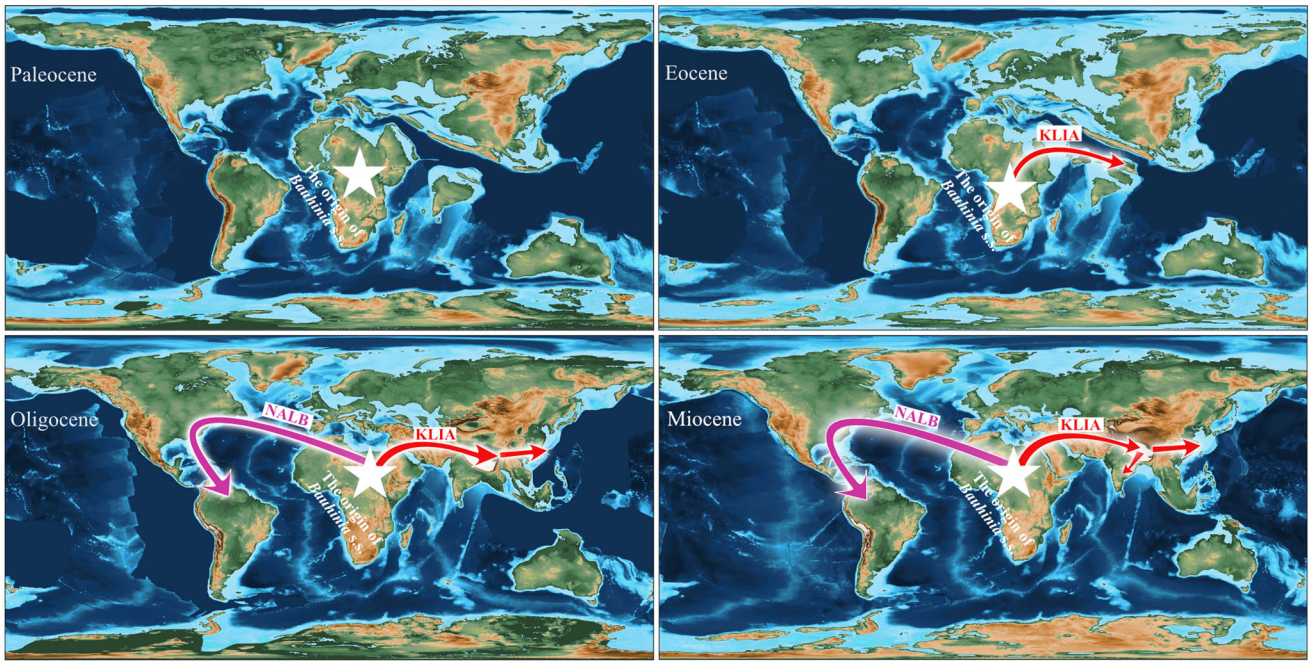

Figure 8. The dispersal routes of *Bauhinia* s.s.

Although no early fossil evidence of *Bauhinia* s.s. has been found in Africa, phylogenetic analyses strongly suggest that the ancestral taxa of *Bauhinia* s.s. likely originated in the Afrotropical realm. The Kohistan-Ladakh Island Arc, recognized as a significant dispersal pathway from Africa to the Indian plate during the Late Cretaceous to the Paleocene, aligns with our findings, as our fossil discovery lies within this pathway (Ali & Aitchison, 2008; Ashton et al., 2021; Chatterjee et al., 2013; Morley, 2018; Smith et al., 2016). Hence, we considered the Kohistan-Ladakh Island Arc as an ancient corridor between Africa and India for *Bauhinia* s.s. from the late Paleocene onwards. We have discovered late Eocene fossils in the Wenshan (Jia et al., 2022), Oligocene fossils in the Ningming (Chen & Zhang, 2005; Wang et al., 2014), and Miocene fossils of *Bauhinia* s.s. in Fujian (Jacques et al., 2015; Lin et al., 2015). All these fossil findings are consistent with our phylogenetic analysis, suggesting that *Bauhinia* s.s. spread eastwards from Lazi by the Eocene, reaching south-eastern China by the Oligocene. Besides, only Miocene fossil records of *Bauhinia* s.s. were found in India, indicating its relatively late dispersal from the southern Tibetan region to northern India. In the Americas, there is a single Miocene fossil record of *Bauhinia* s.s. (Berry, 1945), which aligns with our hypothesis that it spread to the Neotropical realm after the early Oligocene. However, further fossil evidence is still needed to bolster our hypothesis.

Above all, we suggest two main routes for the biogeographic history of *Bauhinia* s.s. during the Paleogene: (1) the Asian clade, to which our fossils belong, originated from the Afrotropical realm before moving to India via the Kohistan-Ladakh Island Arc and later spread to south-eastern China during the Oligocene and to southern India in the Neogene or earlier period; and (2) the American clade originated from the Afrotropical realm and spread to the Neotropical realm via the North Atlantic Land Bridge.

The floristic status of the Tibetan region in the Paleogene

During the Paleogene, multiple lines of fossil evidence confirmed that the Tibetan region was a crossroads for floristic interchange, and the tectonic evolution of this region was an important factor for the formation of species diversity in Asia (Ding et al., 2020; Zhou et al., 2023). In addition to *B. tibetensis* described in this study, there are also plenty of currently known earliest fossil records worldwide found in the central Tibetan region, e.g. *Asclepiadospermum marginatum* (Del Rio et al., 2020; Su et al., 2020), as well as the earliest fossil records in Asia, e.g. *Limnobiophyllum pedunculatum* (Low et al., 2020), *Illigera eocenica* (Wang et al., 2021) and *Koelreuteria kvacekii* (Chen et al., 2022). Thus, the Tibetan region is a pivotal region for the origin, dispersal, and migration of many taxa.

The India-Asia collision process occurred during the early Paleocene (Ding et al., 2014, 2017; Yuan et al., 2022). At approximately 55–50 Ma, the Lazi region, now in the southern Tibetan region, was rich in plant diversity, and many plants survived at low elevation together with *Bauhinia* s.s., e.g. *Livistona*, *Annona* and *Ficus* (Fang et al., 2005; Tao et al., 1988). Ding et al. (2017) used the Climate-Leaf Analysis Multivariate Program (CLAMP) to reconstruct the palaeoenvironment of the Liuqu flora, which suggested that during the late Paleocene, the Lazi region was still at a relatively low altitude (∼1000 m or even lower) with a mean annual temperature of ∼23.8 °C and a growing season precipitation was approximately 2205 mm, and specific humidity (SH) was 13.5 g/kg. The warm and humid condition there fitted the climate requirements of *Bauhinia* s.s. Accompanying the rise of the southern Tibetan region, the climate changed dramatically, and the biodiversity reorganized and decreased significantly (Zhou et al., 2023). *Bauhinia* s.s. could not survive at such high altitudes but survived at lower latitudes nearby. Therefore, the discovery of *B. tibetensis* supports the importance of fossil records in biogeographic studies, especially those from regions outside their modern distribution (Su et al., 2020).

Conclusions

We report the oldest fossil record of *Bauhinia* s.s., namely *Bauhinia tibetensis* Y. Gao and T. Su sp. nov. from the latest Paleocene of the southern Tibetan region. Together with phylogenetic analyses, the results suggest that *Bauhinia* s.s. originated from Africa and spread into what is now the southern Tibetan Plateau by the late Paleocene, after which the Asian clade began to diverge. The collision and convergence of the Indian and Eurasian plates opened a two-way path for floristic interchange between the Indian Plate and the Tibetan region. With the uplift of the Himalayan orogenic belt, suitable habitats for *Bauhinia* s.s. gradually disappeared. Then, the Asian clade migrated southwards and spread into warm and humid regions at low latitudes. The dispersal routes of *Bauhinia* s.s. support the hypothesis that the Tibetan region was an ancient crossroads for biotic interchange during the Paleogene.

Acknowledgements

We thank the members of the Paleoecology Research Group from Xishuangbanna Tropical Botanical Garden, Chinese Academy of Sciences (CAS) and colleagues from Kunming Institute of Botany, CAS for fossil collection works. We thank the Institutional Center for Shared Technologies and Facilities of Xishuangbanna Tropical Botanical Garden, CAS for providing imaging equipment and assisting with fossil scans. This work is supported by the National Key Research and Development Program (2022YFF0800800), the Second Tibetan Plateau Scientific Expedition program (2019QZKK0705), the National Natural Science Foundation of China (NSFC) (41988101), the Strategic Priority Research Program of the Chinese Academy of Sciences (CAS) (XDB26000000), the Youth Innovation Promotion Association, CAS (Y2021105), and the Basic Research Project in Yunnan (YNWR-QNBJ-2019-086).

Disclosure statement

No potential conflict of interest was reported by the author(s).

Supplemental material

Supplemental material for this article can be accessed here: http://dx.doi.org/10.1080/14772019.2023.2244495.

References

Adams, D. C., **Collyer, M.**, & **Kaliontzopoulou, A.** (2020). Package 'geomorph': Geometric morphometric analyses of 2D/3D landmark data. https://github.com/geomorphR/geomorph/

Akli, A., **Lorenzo, Z.**, **Alía, R.**, **Rabhi, K.**, & **Torres, E.** (2022). Morphometric analyses of leaf shapes in four sympatric Mediterranean oaks and hybrids in the Algerian kabylie forest. *Forests*, *13*, 508. https://doi.org/10.3390/f13040508

Ali, J. R., & **Aitchison, J. C.** (2008). Gondwana to Asia: plate tectonics, paleogeography and the biological connectivity of the Indian sub-continent from the Middle Jurassic through Latest Eocene (166–35 Ma). *Earth-Science Reviews*, *88*, 145–166. https://doi.org/10.1016/j.earscirev.2008.01.007

Ashton, P. S., **Morley, R. J.**, **Heckenhauer, J.**, & **Prasad, V.** (2021). The magnificent Dipterocarps: Précis for an epitaph? *Kew Bulletin*, *76*, 87–125. https://doi.org/10.1007/s12225-021-09934-7

Awasthi, N., & **Mehrotra, R.** (1989). Some fossil woods from Tipam Sandstone of Assam and Nagaland. *Journal of Palaeosciences*, *38*, 277–284. https://doi.org/10.54991/jop.1989.1662

Awasthi, N., & **Prasad, M.** (1989). Siwalik plant fossils from Surai Khola area, western Nepal. *Journal of Palaeosciences*, *38*, 298–318. https://doi.org/10.54991/jop.1989.1665

Bande, M., & **Srivastava, G.** (1988). Late Cenozoic plant-impressions from Mahuadanr valley, Palamu District, Bihar. *Journal of Palaeosciences*, *37*, 331–366. https://doi.org/10.54991/jop.1988.1632

Bansal, M., **Morley, R. J.**, **Nagaraju, S. K.**, **Dutta, S.**, **Mishra, A. K.**, **Selveraj, J.**, **Kumar, S.**, **Niyolia, D.**, **Harish, S. M.**, **Abdelrahim, O. B.**, **Hasan, S. E.**,

Ramesh, B. R., **Dayanandan, S.**, **Morley, H. P.**, **Ashton, P. S.**, & **Prasad, V.** (2022). Southeast Asian Dipterocarp origin and diversification driven by Africa-India floristic interchange. *Science*, *375*, 455–460. https://doi.org/10.1126/science.abk2177

Berry, E. (1945). Fossil floras from southern Ecuador. *Johns Hopkins University Studies in Geology*, *14*, 93–150.

Bookstein, F. L. (1997). Landmark methods for forms without landmarks: Morphometrics of group differences in outline shape. *Medical Image Analysis*, *1*, 225–243. https://doi.org/10.1016/S1361-8415(97)85012-8

Bromhead, E. F. (1838). An attempt to ascertain characters of the botanical alliances. *The Edinburgh New Philosophical Journal*, *25*, 123–134.

Calvillo-Canadell, L., & **Cevallos-Ferriz, S. R. S.** (2002). *Bauhcis moranii* gen. et sp. nov. (Cercideae, Caesalpinieae), an Oligocene plant from Tepexi de Rodríguez, Puebla, Mex., with leaf architecture similar to *Bauhinia* and *Cercis*. *Review of Palaeobotany and Palynology*, *122*, 171–184. https://doi.org/10.1016/S0034-6667(02)00135-5

Chaney, R. W. (1933). A Tertiary flora from Uganda. *The Journal of Geology*, *41*, 702–709. https://doi.org/10.1086/624089

Chatterjee, S., **Goswami, A.**, & **Scotese, C. R.** (2013). The longest voyage: Tectonic, magmatic, and paleoclimatic evolution of the Indian plate during its northward flight from Gondwana to Asia. *Gondwana Research*, *23*, 238–267. https://doi.org/10.1016/j.gr.2012.07.001

Chen, L., **Deng, W.**, **Su, T.**, **Li, S.**, & **Zhou, Z.** (2021). Late Eocene sclerophyllous oak from Markam Basin, Tibet, and its biogeographic implications. *Science China Earth Sciences*, *64*, 1969–1981. https://doi.org/10.1007/s11430-020-9826-4

Chen, P.-R., **Del Rio, C.**, **Huang, J.**, **Liu, J.**, **Zhao, J.-G.**, **Spicer, R. A.**, **Li, S.-F.**, **Wang, T.-X.**, **Zhou, Z.-K.**, & **Su, T.** (2022). Fossil capsular valves of *Koelreuteria* (Sapindaceae) from the Eocene of Central Tibetan Plateau and Their Biogeographic Implications. *International Journal of Plant Sciences*, *183*, 307–319. https://doi.org/10.1086/719401

Chen, Y., & **Zhang, D.-X.** (2005). *Bauhinia larsenii*, a fossil legume from Guangxi, China. *Botanical Journal of the Linnean Society*, *147*, 437–440. https://doi.org/10.1111/j.1095-8339.2005.00373.x

Davis, C. C., **Bell, C. D.**, **Mathews, S.**, & **Donoghue, M. J.** (2002). Laurasian migration explains Gondwanan disjunctions: Evidence from Malpighiaceae. *Proceedings of the National Academy of Sciences*, *99*, 6833–6837. https://doi.org/10.1073/pnas.102175899

de Candolle, A. P. (1825). *Prodromus systematis naturalis regni vegetabilis, sive, Enumeratio contracta ordinum generum specierumque plantarum huc usque cognitarium, juxta methodi naturalis, normas digesta*. Sumptibus Sociorum Treuttel et Würtz.

de Jussieu, A. L. (1789). *Antonii Laurentii de Jussieu genera plantarum: Secundum ordines naturales disposita, juxta methodum in horto regio parisiensi exaratam*. Herissant et Theophilum Barrois.

Del Rio, C., **Wang, T.**, **Liu, J.**, **Liang, S.**, **Spicer, R. A.**, **Wu, F.**, **Zhou, Z.**, & **Su, T.** (2020). *Asclepiadospermum* gen. nov., the earliest fossil record of Asclepiadoideae (Apocynaceae) from the Early Eocene of central Qinghai-Tibetan Plateau, and its biogeographic implications. *American Journal of Botany*, *107*, 126–138. https://doi.org/10.1002/ajb2.1418

Deng, T., **Wu, F.**, **Zhou, Z.**, & **Su, T.** (2020). Tibetan Plateau: An evolutionary junction for the history of modern biodiversity. *Science China Earth Sciences*, *63*, 172–187. https://doi.org/10.1007/s11430-019-9507-5

Ding, L., **Xu, Q.**, **Yue, Y.**, **Wang, H.**, **Cai, F.**, & **Li, S.** (2014). The Andean-type Gangdese Mountains: Paleoelevation record from the Paleocene–Eocene Linzhou Basin. *Earth and Planetary Science Letters*, *392*, 250–264. https://doi.org/10.1016/j.epsl.2014.01.045

Ding, L., **Spicer, R. A.**, **Yang, J.**, **Xu, Q.**, **Cai, F.**, **Li, S.**, **Lai, Q.**, **Wang, H.**, **Spicer, T. E. V.**, **Yue, Y.**, **Shukla, A.**, **Srivastava, G.**, **Khan, M. A.**, **Bera, S.**, & **Mehrotra, R.** (2017). Quantifying the rise of the Himalaya orogen and implications for the South Asian monsoon. *Geology*, *45*, 215–218. https://doi.org/10.1130/G38583.1

Ding, W.-N., **Ree, R. H.**, **Spicer, R. A.**, & **Xing, Y.-W.** (2020). Ancient orogenic and monsoon-driven assembly of the world's richest temperate alpine flora. *Science*, *369*, 578–581. https://doi.org/10.1126/science.abb4484

Ellis, B., **Daly, D. C.**, **Hickey, L. J.**, **Johnson, K. R.**, **Mitchell, J. D.**, **Wilf, P.**, & **Wing, S. L.** (2009). *Manual of Leaf Architecture*. Cornell University Press.

Fang, A., **Yan, Z.**, **Liu, X.**, **Tao, J.**, **Li, J.**, & **Pan, Y.** (2005). The flora of the Liuqu Formation in south Tibet and its climatic implications. *Acta Palaeontologica Sinica*, *44*, 442. https://doi.org/10.3724/SP.J.1006.2018.00442

Guleria, J., **Srivastava, R.**, & **Prasad, M.** (2000). Some fossil leaves from the Kasauli Formation of Himachal Pradesh, north-west India. *Himalayan Geology*, *21*, 43–52.

Hickey, L. J. (1973). Classification of the architecture of dicotyledonous leaves. *American Journal of Botany*, *60*, 17–33. https://doi.org/10.1002/j.1537-2197.1973.tb10192.x

Hijmans, R. J., **Van Etten, J.**, **Sumner, M.**, **Cheng, J.**, **Baston, D.**, **Bevan, A.**, **Bivand, R.**, **Busetto, L.**, **Canty, M.**, & **Fasoli, B.** (2020). *Raster: Geographic data analysis and modeling* (R package version, 2–1).

Jacques, F. M. B., **Shi, G.**, **Su, T.**, & **Zhou, Z.** (2015). A tropical forest of the Middle Miocene of Fujian (SE China) reveals Sino-Indian biogeographic affinities. *Review of Palaeobotany and Palynology*, *216*, 76–91. https://doi.org/10.1016/j.revpalbo.2015.02.001

Jia, L.-B., **Hu, J.-J.**, **Zhang, S.-T.**, **Su, T.**, **Spicer, R. A.**, **Liu, J.**, **Yang, J.-C.**, **Zou, P.**, **Huang, Y.-J.**, & **Zhou, Z.-K.** (2022). *Bauhinia* (Leguminosae) fossils from the Paleogene of southwestern China and its species accumulation in Asia. *Diversity*, *14*, 173. https://doi.org/10.3390/d14030173

Kalyaanamoorthy, S., **Minh, B. Q.**, **Wong, T. K. F.**, **von Haeseler, A.**, & **Jermiin, L. S.** (2017). ModelFinder: Fast model selection for accurate phylogenetic estimates. *Nature Methods*, *14*, 587–589. https://doi.org/10.1038/nmeth.4285

Khan, M. A., **Bera, M.**, **Spicer, R. A.**, **Spicer, T. E. V.**, & **Bera, S.** (2019). Floral diversity and environment during the middle Siwalik sedimentation (Pliocene) in the Arunachal sub-Himalaya. *Palaeobiodiversity and Palaeoenvironments*, *99*, 401–424. https://doi.org/10.1007/s12549-018-0351-2

Klein, L., & **Svoboda, H.** (2017). Comprehensive methods for leaf geometric morphometric analyses. *Bio-Protocol*, *7*, e2269–e2269. https://doi.org/10.21769/bioprotoc.2269

Klingenberg, C. P. (2022). Methods for studying allometry in geometric morphometrics: A comparison of performance. *Evolutionary Ecology*, *36*, 439–470. https://doi.org/10.1007/s10682-022-10170-z

Lakhanpal, R. N., & **Guleria, J. S.** (1982). Plant remains from the Miocene of Kachchh, Western India. *Journal of Palaeosciences*, *30*, 279–296. https://doi.org/10.54991/jop.1982.1455

Larkin, M. A., **Blackshields, G.**, **Brown, N. P.**, **Chenna, R.**, **McGettigan, P. A.**, **McWilliam, H.**, **Valentin, F.**, **Wallace, I. M.**, **Wilm, A.**, **Lopez, R.**, **Thompson, J. D.**, **Gibson, T. J.**, & **Higgins, D. G.** (2007). Clustal W and Clustal X version 2.0. *Bioinformatics*, *23*, 2947–2948. https://doi.org/10.1093/bioinformatics/btm404

Larsson, A. (2014). AliView: a fast and lightweight alignment viewer and editor for large datasets. *Bioinformatics*, *30*, 3276–3278. https://doi.org/10.1093/bioinformatics/btu531

Leary, R. J., **DeCelles, P. G.**, **Quade, J.**, **Gehrels, G. E.**, & **Waanders, G.** (2016). The Liuqu Conglomerate, southern Tibet: Early Miocene basin development related to deformation within the Great Counter Thrust system. *Lithosphere*, *8*, 427–450. https://doi.org/10.1130/L542.1

Leary, R. J., **Quade, J.**, **DeCelles, P. G.**, & **Reynolds, A.** (2017). Evidence from paleosols for low to moderate elevation of the India–Asia suture zone during mid-Cenozoic time. *Geology*, *45*, 399–402. https://doi.org/10.1130/G38830.1

Li, G., **Kohn, B.**, **Sandiford, M.**, **Xu, Z.**, & **Wei, L.** (2015). Constraining the age of Liuqu Conglomerate, southern Tibet: Implications for evolution of the India–Asia collision zone. *Earth and Planetary Science Letters*, *426*, 259–266. https://doi.org/10.1016/j.epsl.2015.06.010

Lin, Y., **Wong, W. O.**, **Shi, G.**, **Shen, S.**, & **Li, Z.** (2015). Bilobate leaves of *Bauhinia* (Leguminosae, Caesalpinioideae, Cercideae) from the Middle Miocene of Fujian Province, southeastern China and their biogeographic implications. *BMC Evolutionary Biology*, *15*, 252. https://doi.org/10.1186/s12862-015-0540-9

Linnaeus, C. (1753). *Species plantarum* (1st ed.). Laurentius Salvius.

Liu, J., **Su, T.**, **Spicer, R. A.**, **Tang, H.**, **Deng, W.-Y.-D.**, **Wu, F.-X.**, **Srivastava, G.**, **Spicer, T.**, **Van Do, T.**, **Deng, T.**, & **Zhou, Z.-K.** (2019). Biotic interchange through lowlands of Tibetan Plateau suture zones during Paleogene. *Palaeogeography, Palaeoclimatology, Palaeoecology*, *524*, 33–40. https://doi.org/10.1016/j.palaeo.2019.02.022

Low, S. L., **Su, T.**, **Spicer, T. E. V.**, **Wu, F.-X.**, **Deng, T.**, **Xing, Y.-W.**, & **Zhou, Z.-K.** (2020). Oligocene *Limnobiophyllum* (Araceae) from the central Tibetan Plateau and its evolutionary and palaeoenvironmental implications. *Journal of Systematic Palaeontology*, *18*, 415–431. https://doi.org/10.1080/14772019.2019.1611673

Mak, C. Y., **Cheung, K. S.**, **Yip, P. Y.**, & **Kwan, H. S.** (2008). Molecular evidence for the hybrid origin of *Bauhinia blakeana* (Caesalpinioideae). *Journal of Integrative Plant Biology*, *50*, 111–118. https://doi.org/10.1111/j.1744-7909.2007.00591.x

Matzke, N. J. (2014). Model selection in historical biogeography reveals that founder-event speciation is a crucial process in island clades. *Systematic Biology*, *63*, 951–970. https://doi.org/10.1093/sysbio/syu056

Mehrotra, R. C., **Bera, S. K.**, **Basumatary, S. K.**, & **Srivastava, G.** (2011). Study of fossil wood from the Middle–Late Miocene sediments of Dhemaji and Lakhimpur districts of Assam, India and its palaeoecological and palaeophytogeographical implications. *Journal of Earth System Science*, *120*, 681–701. https://doi.org/10.1007/s12040-011-0103-4

Meng, H.-H., **Jacques, F. M.**, **Su, T.**, **Huang, Y.-J.**, **Zhang, S.-T.**, **Ma, H.-J.**, & **Zhou, Z.-K.** (2014). New biogeographic insight into *Bauhinia* s.l. (Leguminosae): Integration from fossil records and molecular analyses. *BMC Evolutionary Biology*, *14*, 181. https://doi.org/10.1186/s12862-014-0181-4

Morley, R. J. (2018). Assembly and division of the South and South-East Asian flora in relation to tectonics and climate change. *Journal of Tropical Ecology*, *34*, 209–234. https://doi.org/10.1017/S0266467418000202

Olson, D. M., **Dinerstein, E.**, **Wikramanayake, E. D.**, **Burgess, N. D.**, **Powell, G. V. N.**, **Underwood, E. C.**, **D'amico, J. A.**, **Itoua, I.**, **Strand, H. E.**, **Morrison, J. C.**, **Loucks, C. J.**, **Allnutt, T. F.**, **Ricketts, T. H.**, **Kura, Y.**, **Lamoreux, J. F.**, **Wettengel, W. W.**, **Hedao, P.**, & **Kassem, K. R.** (2001). Terrestrial ecoregions of the world: A new map of life on earth. *BioScience*, *51*, 933. https://doi.org/10.1641/0006-3568(2001)051[0933:TEOTWA]2.0.CO;22.0.CO;2]

Prakash, U., & **Prasad, M.** (1984). Wood of Bauhinia from the Siwalik beds of Uttar Pradesh, India. *Journal of Palaeosciences*, *32*, 140–145. https://doi.org/10.54991/jop.1984.1372

Rapini, A., **Chase, M. W.**, **Goyder, D. J.**, & **Griffiths, J.** (2003). Asclepiadeae classification: evaluating the phylogenetic relationships of New World Asclepiadoideae (Apocynaceae). *Taxon*, *52*, 33–50. https://doi.org/10.2307/3647436

Rohlf, F. (2015). The tps series of software. *Hystrix, the Italian Journal of Mammalogy*, *26*, 9–12. https://doi.org/10.4404/hystrix-26.1-11264

Scotese, C. (2016). *PALEOMAP PaleoAtlas for GPlates and the PaleoData plotter program*. *PALEOMAP project*. https://doi.org/10.13140/RG.2.2.34367.00166

Shukla, A., **Mehrotra, R. C.**, **Mandal, N.**, & **Thakkar, M. G.** (2015). Two new fossil woods from the Early Miocene of Kutch, Gujarat, India and their significance. *Historical Biology*, *27*, 970–977. https://doi.org/10.1080/08912963.2014.917088

Sinou, C., **Cardinal-McTeague, W.**, & **Bruneau, A.** (2020). Testing generic limits in Cercidoideae (Leguminosae): insights from plastid and duplicated nuclear gene sequences. *Taxon*, *69*, 67–86. https://doi.org/10.1002/tax.12207

Sinou, C., **Forest, F.**, **Lewis, G. P.**, & **Bruneau, A.** (2009). The genus *Bauhinia* s.l. (Leguminosae): A phylogeny based on the plastid *trn*L–*trn*F region. *Botany*, *87*, 947–960. https://doi.org/10.1139/B09-065

Smith, T., **Kumar, K.**, **Rana, R. S.**, **Folie, A.**, **Solé, F.**, **Noiret, C.**, **Steeman, T.**, **Sahni, A.**, & **Rose, K. D.** (2016). New Early Eocene vertebrate assemblage from western India reveals a mixed fauna of European and Gondwana affinities. *Geoscience Frontiers*, *7*, 969–1001. https://doi.org/10.1016/j.gsf.2016.05.001

Spicer, R. A., **Su, T.**, **Valdes, P. J.**, **Farnsworth, A.**, **Wu, F.-X.**, **Shi, G.**, **Spicer, T. E. V.**, & **Zhou, Z.** (2021). Why 'the uplift of the Tibetan Plateau' is a myth. *National Science Review*, *8*, nwaa091. https://doi.org/10.1093/nsr/nwaa091

Steven J. Phillips, **Miroslav Dudík**, **Robert E. Schapire**. (2022). *Maxent software for modeling species niches and distributions* (Version 3.4.1). http://biodiversityinformatics.amnh.org/open_source/maxent/

Stojnić, S., **Viscosi, V.**, **Marković, M.**, **Ivanković, M.**, **Orlović, S.**, **Tognetti, R.**, **Cocozza, C.**, **Vasić, V.**, & **Loy, A.** (2022). Spatial patterns of leaf shape variation in

European beech (*Fagus sylvatica* L.) provenances. *Trees*, *36*, 497–511. https://doi.org/10.1007/s00468-021-02224-6

Su, T., **Spicer, R. A.**, **Wu, F.-X.**, **Farnsworth, A.**, **Huang, J.**, **Del Rio, C.**, **Deng, T.**, **Ding, L.**, **Deng, W.-Y.-D.**, **Huang, Y.-J.**, **Hughes, A.**, **Jia, L.-B.**, **Jin, J.-H.**, **Li, S.-F.**, **Liang, S.-Q.**, **Liu, J.**, **Liu, X.-Y.**, **Sherlock, S.**, **Spicer, T.**, **Srivastava, G.**, **Tang, H.**, **Valdes, P.**, **Wang, T.-X.**, **Widdowson, M.**, **Wu, M.-X.**, **Xing, Y.-W.**, **Xu, C.-L.**, **Yang, J.**, **Zhang, C.**, **Zhang, S.-T.**, **Zhang, X.-W.**, **Zhao, F.**, & **Zhou, Z.-K.** (2020). A Middle Eocene lowland humid subtropical "Shangri-La" ecosystem in central Tibet. *Proceedings of the National Academy of Sciences*, *117*, 32989–32995. https://doi.org/10.1073/pnas.2012647117

Suchard, M. A., **Lemey, P.**, **Baele, G.**, **Ayres, D. L.**, **Drummond, A. J.**, & **Rambaut, A.** (2018). Bayesian phylogenetic and phylodynamic data integration using BEAST 1.10. *Virus Evolution*, *4*(1), vey016. https://doi.org/10.1093/ve/vey016

Tao, J., **Whyte, P.**, **Aigner, J.**, **Jablonski, N.**, **Taylor, G.**, **Walker, D.**, & **Wang, P.** (1988). The Paleogene flora and palaeoclimate of Liuqu Formation in Xizang (Tibet). *The Paleoenvironment of East Asia from the Mid-Tertiary: University of Hong Kong*, *Hong Kong, Centre of Asian Studies Occasional Papers and Monographs*, *77*, 520–522.

Tian, Y., **Spicer, R. A.**, **Huang, J.**, **Zhou, Z.**, **Su, T.**, **Widdowson, M.**, **Jia, L.**, **Li, S.**, **Wu, W.**, **Xue, L.**, **Luo, P.**, & **Zhang, S.** (2021). New Early Oligocene zircon U-Pb dates for the 'Miocene' Wenshan Basin, Yunnan, China: Biodiversity and paleoenvironment. *Earth and Planetary Science Letters*, *565*, 116929. https://doi.org/10.1016/j.epsl.2021.116929

Valdes, P. J., **Armstrong, E.**, **Badger, M. P. S.**, **Bradshaw, C. D.**, **Bragg, F.**, **Crucifix, M.**, **Davies-Barnard, T.**, **Day, J. J.**, **Farnsworth, A.**, **Gordon, C.**, **Hopcroft, P. O.**, **Kennedy, A. T.**, **Lord, N. S.**, **Lunt, D. J.**, **Marzocchi, A.**, **Parry, L. M.**, **Pope, V.**, **Roberts, W. H. G.**, **Stone, E. J.**, **Tourte, G. J. L.**, & **Williams, J. H. T.** (2017). The BRIDGE HadCM3 family of climate models: HadCM3@Bristol v1.0. *Geoscientific Model Development*, *10*, 3715–3743. https://doi.org/10.5194/gmd-10-3715-2017

Valdes, P. J., **Scotese, C. R.**, & **Lunt, D. J.** (2021). Deep ocean temperatures through time. *Climate of the Past*, *17*, 1483–1506. https://doi.org/10.5194/cp-17-1483-2021

Wang, Q., **Song, Z.**, **Chen, Y.**, **Shen, S.**, & **Li, Z.** (2014). Leaves and fruits of *Bauhinia* (Leguminosae, Caesalpinioideae, Cercideae) from the Oligocene Ningming Formation of Guangxi, South China and their biogeographic implications. *BMC Evolutionary Biology*, *14*, 88. https://doi.org/10.1186/1471-2148-14-88

Wang, T., **Del Rio, C.**, **Manchester, S. R.**, **Liu, J.**, **Wu, F.**, **Deng, W.**, **Su, T.**, & **Zhou, Z.** (2021). Fossil fruits of *Illigera* (Hernandiaceae) from the Eocene of central Tibetan Plateau. *Journal of Systematics and Evolution*, *59*, 1276–1286. https://doi.org/10.1111/jse.12687

Westerhold, T., **Marwan, N.**, **Drury, A. J.**, **Liebrand, D.**, **Agnini, C.**, **Anagnostou, E.**, **Barnet, J. S. K.**, **Bohaty, S. M.**, **De Vleeschouwer, D.**, **Florindo, F.**, **Frederichs, T.**, **Hodell, D. A.**, **Holbourn, A. E.**, **Kroon, D.**, **Lauretano, V.**, **Littler, K.**, **Lourens, L. J.**, **Lyle, M.**, **Pälike, H.**, **Röhl, U.**, **Tian, J.**, **Wilkens, R. H.**, **Wilson, P. A.**, & **Zachos, J. C.** (2020). An astronomically dated record of Earth's climate and its predictability over the last 66 million years. *Science*, *369*, 1383–1387. https://doi.org/10.1126/science.aba6853

Xu, C., **Su, T.**, **Huang, J.**, **Huang, Y.**, **Li, S.**, **Zhao, Y.**, & **Zhou, Z.** (2019). Occurrence of *Christella* (Thelypteridaceae) in Southwest China and its indications of the paleoenvironment of the Qinghai–Tibetan Plateau and adjacent areas. *Journal of Systematics and Evolution*, *57*, 169–179. https://doi.org/10.1111/jse.12452

Yang, K., **Wu, J.**, **Li, X.**, **Pang, X.**, **Yuan, Y.**, **Qi, G.**, & **Yang, M.** (2022). Intraspecific leaf morphological variation in *Quercus dentata* Thunb.: A comparison of traditional and geometric morphometric methods, a pilot study. *Journal of Forestry Research*, *33*, 1751–1764. https://doi.org/10.1007/s11676-022-01452-x

Yu, Y., **Blair, C.**, & **He, X.** (2020). RASP 4: Ancestral state reconstruction tool for multiple genes and characters. *Molecular Biology and Evolution*, *37*, 604–606. https://doi.org/10.1093/molbev/msz257

Yuan, J., **Deng, C.**, **Yang, Z.**, **Krijgsman, W.**, **Thubtantsering , Qin, H.**, **Shen, Z.**, **Hou, Y.**, **Zhang, S.**, **Yu, Z.**, **Zhao, P.**, **Zhao, L.**, **Wan, B.**, **He, H.**, & **Guo, Z.** (2022). Triple-stage India-Asia collision involving arc-continent collision and subsequent two-stage continent-continent collision. *Global and Planetary Change*, *212*, 103821. https://doi.org/10.1016/j.gloplacha.2022.103821

Zachos, J. C., **Shackleton, N. J.**, **Revenaugh, J. S.**, **Pälike, H.**, & **Flower, B. P.** (2001). Climate response to orbital forcing across the Oligocene-Miocene boundary. *Science*, *292*, 274–278. https://doi.org/10.1126/science.1058288

Zhang, D., **Gao, F.**, **Jakovlić, I.**, **Zou, H.**, **Zhang, J.**, **Li, W. X.**, & **Wang, G. T.** (2020). PhyloSuite: An integrated and scalable desktop platform for streamlined molecular sequence data management and evolutionary phylogenetics studies. *Molecular Ecology Resources*, *20*, 348–355. https://doi.org/10.1111/1755-0998.13096

Zhang, Z., **Ramstein, G.**, **Schuster, M.**, **Li, C.**, **Contoux, C.**, & **Yan, Q.** (2014). Aridification of the Sahara desert caused by Tethys sea shrinkage during the Late Miocene. *Nature*, *513*, 401–404. https://doi.org/10.1038/nature13705

Zhao, Y., **Zhang, R.**, **Jiang, K.-W.**, **Qi, J.**, **Hu, Y.**, **Guo, J.**, **Zhu, R.**, **Zhang, T.**, **Egan, A. N.**, **Yi, T.-S.**, **Huang, C.-H.**, & **Ma, H.** (2021). Nuclear phylotranscriptomics and phylogenomics support numerous polyploidization events and hypotheses for the evolution of rhizobial nitrogen-fixing symbiosis in Fabaceae. *Molecular Plant*, *14*, 748–773. https://doi.org/10.1016/j.molp.2021.02.006

Zhou, Z., **Liu, J.**, **Chen, L.**, **Spicer, R. A.**, **Li, S.**, **Huang, J.**, **Zhang, S.**, **Huang, Y.**, **Jia, L.**, **Hu, J.**, & **Su, T.** (2023). Cenozoic plants from Tibet: An extraordinary decade of discovery, understanding and implications. *Science China Earth Sciences*, *66*, 205–226. https://doi.org/10.1007/s11430-022-9980-9

Zhou, Z., **Wang, T.**, **Huang, J.**, **Liu, J.**, **Deng, W.**, **Li, S.**, **Deng, C.**, & **Su, T.** (2020). Fossil leaves of *Berhamniphyllum* (Rhamnaceae) from Markam, Tibet and their biogeographic implications. *Science China Earth Sciences*, *63*, 224–234. https://doi.org/10.1007/s11430-019-9477-8

Zhou, Z., **Yang, X.**, & **Yang, Q.** (2006). Land bridge and long-distance dispersal—Old views, new evidence. *Chinese Science Bulletin*, *51*, 1030–1038. https://doi.org/10.1007/s11434-006-1030-7

Associate Editor: Paul Kenrick